received signals were unchanged since these frequencies were already above the penetration frequency. At 1.7 MHz, however, the transition occurred from no reception to reception. This is consistent with earlier observations that showed that the galactic signal normally begins leaking through the ionosphere when f_oF_2 falls to within about 100 kHz of the receiver frequency (*14*). The signal reached a maximum at 0540 hours and then slowly decreased until sunrise caused f_oF_2 to rise near 0700 hours. The profile from 0540 to 0640 hours was generally similar to that at 2.108 MHz and to the corresponding variation seen at the same right ascension in previous observations at 2.13 MHz (*17*) and may be taken to represent the galactic brightness distribution of declination $-43°$ and right ascension of 0200 to 0300 hours. This is the first observation of this region at 1.7 MHz with 25° resolution, the nearest similar measurements having been made with the lunar-orbiting spacecraft RAE-2 at 1.3 MHz and with 130° resolution (*18*).

Figure 5C shows the spectrum of the galactic background radio emission derived from the observations at 0630 local time (galactic coordinates $\ell = 220°$, $b = -52°$). The spectrum observed by the RAE-2 spacecraft is shown for comparison. The flux measurement labeled (a) at 1.704 MHz represents the view through the "ionospheric hole" associated with the shuttle-induced plasma depletion. Observations over a period of several weeks before and after the experiment failed to produce any comparable records at 1.704 MHz since the natural ionospheric cutoff frequency never approached the low values associated with the Spacelab-2 "ionospheric hole" experiment.

The Millstone Hill experiments provided clear and unambiguous documentation of both the largest and smallest types of ionospheric holes capable of being induced by the space shuttle OMS engines. Although full modeling results are yet to be completed, the observations are essentially consistent with theories before the experiment. The sizes and longevities of the holes were somewhat larger and longer than anticipated, and the airglow patterns still require detailed simulation work to verify the dominant chemistry tracks. The dramatic slippage of the exhaust cloud through the ionosphere demonstrates the need for precise planning for future active experiments requiring gas releases at orbital speeds. In addition, the Hobart experiment succeeded in demonstrating that artificial means can be used to open ionospheric windows for the reception of low-frequency radiation of celestial origin.

REFERENCES AND NOTES

1. M. Mendillo and J. M. Forbes, *J. Geophys. Res.* **83**, 151 (1978).
2. P. A. Bernhardt, *ibid.* **84**, 793 and 4341 (1979).
3. M. Mendillo, *Adv. Space Res.* **1**, 275 (1981).
4. ——, *ibid.*, in press.
5. J. V. Evans, *Proc. IEEE* **57**, 496 (1969).
6. The Millstone 1 nighttime burn occurred from 0322:17 to 0323:04 UT on 30 July 1985 at an altitude of 320 km from 41.6°N, 73.1°W to 40.0°N, 69.8°W.
7. The Millstone 2 daytime burn occurred from 1914:44 to 1914:50 UT on 4 August 1985 at an altitude of 323 km from 40.9°N, 71.5°W to 41.1°N, 71.1°W.
8. M. D. Papagiannis and M. Mendillo, *Nature (London)* **255**, 42 (1975).
9. The Hobart burn occurred from 1659:27 to 1659:43 UT on 4 August 1985 at an altitude of 322 km from −42.4°N, 213.5°W to −42.9°N, 212.3°W.
10. J. Baumgardner and S. Karandanis, *Electron. Imaging* **3**, 28 (1984).
11. A. E. Hedin, *J. Geophys. Res.* **88**, 10170 (1983).
12. H. G. Booker, *ibid.* **66**, 1073 (1961).
13. R. H. Wand and M. Mendillo, *ibid.* **89**, 203 (1984).
14. G. Reber and G. R. A. Ellis, *ibid.* **61**, 1 (1956).
15. G. R. A. Ellis, *Mon. Notices R. Astron. Soc.* **130**, 429 (1965).
16. G. R. A. Ellis *et al.*, *Adv. Space Res.*, in press.
17. G. Reber, *J. Franklin Inst.* **285**, 1 (1967).
18. J. C. Novaco and L. W. Brown, *Astrophys. J.* **221**, 114 (1978).
19. G. R. A. Ellis, *Aust. J. Phys.* **35**, 91 (1982).

20. We thank the Spacelab-2 crew, NASA team members at the Marshall Space Fight Center (with special thanks to S. Perrine and the Orbital Dynamics Group), and many colleagues who contributed to these experiments. Funding for this work came in part from NASA contract NAS8-32844 to Boston University. The Millstone radar program was supported under NSF Cooperative Agreement ATM-84-19117 to the Massachusetts Institute of Technology. The University of Tasmania radio astronomy observations were financed by the Australian Research Grant Scheme.

26 May 1987; accepted 22 September 1987

White Light Sunspot Observations from the Solar Optical Universal Polarimeter on Spacelab-2

R. A. SHINE, A. M. TITLE, T. D. TARBELL, K. P. TOPKA

The flight of the Solar Optical Universal Polarimeter on Spacelab-2 provided the opportunity for the collection of time sequences of diffraction-limited (0.5 arc second) solar images with excellent pointing stability (0.003 arc second) and with freedom from the distortion that plagues ground-based images. A series of white-light images of active region 4682 were obtained on 5 August 1985, and the area containing the sunspot has been analyzed. These data have been digitally processed to remove noise and to separate waves from low-velocity material motions. The results include (i) proper motion measurements of a radial outflow in the photospheric granulation pattern just outside the penumbra; (ii) discovery of occasional bright structures ("streakers") that appear to be ejected outward from the penumbra; (iii) broad dark "clouds" moving outward in the penumbra, in addition to the well-known bright penumbral grains moving inward; (iv) apparent extensions and contractions of penumbral filaments over the photosphere; and (v) observation of a faint bubble or looplike structure that seems to expand from two bright penumbral filaments into the photosphere.

THE SOLAR OPTICAL UNIVERSAL POLARIMETER (SOUP) flew on the space shuttle Challenger as part of the Spacelab-2 mission from 29 July to 6 August 1985. A description of the SOUP instrument and a summary of the data obtained are given by Title *et al.* (*1*). Because of electronic and thermal problems, only the white-light film data were scientifically useful. However, the high resolution (approximately 0.5 arc sec or 350 km) and, more importantly, the stability and freedom from variable atmospheric distortion of these data have provided an unprecedented opportunity to study the dynamics of the solar photosphere by viewing and analyzing movie sequences.

The Spacelab-2 mission was flown during the sunspot minimum of the solar cycle, but we observed a medium-sized sunspot and a group of pores on the disk during the week of the mission. These features were in active region 4682, which was located at Carrington coordinates S15W30 during the SOUP observations. The region and the major sunspot were decaying. Images containing the sunspot in the field of view were obtained during portions of five orbits. The longest uninterrupted sequence was exposed during orbit 110 and consists of about 28 minutes of data with a frame taken every 2 seconds on 5 August 1985 between 1910 and 1938 Greenwich mean time. Analysis of data from the image stabilization system indicates a root mean square jitter of only

Lockheed Palo Alto Research Laboratory, Palo Alto, CA 94304.

0.003 arc sec. In this report we have used this particular sequence in all of the analysis. We have digitized every fifth frame over the entire interval to give us data with 10-second spacing. The sunspot umbra was underexposed, but the penumbra and the surrounding photosphere show a large variety of interesting phenomena, many not previously described. Figure 1 shows a processed SOUP image of the sunspot together with a diagram that indicates the locations of some of these phenomena.

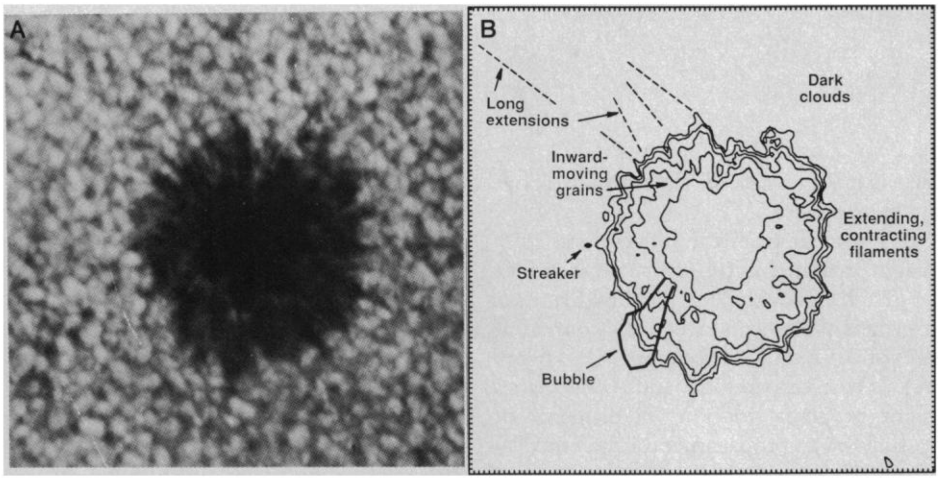

Fig. 1. (**A**) A sunspot image from the SOUP instrument. This is a single frame from a movie that was processed by means of a three-dimensional Fourier filter that zeroed all Fourier components in transform space with phase velocities greater than 4 km/sec. High spatial frequencies were also enhanced to improve contrast. (**B**) A contour diagram indicating locations of various phenomena. The tick marks are spaced at 1-arc-sec intervals (≈725 km).

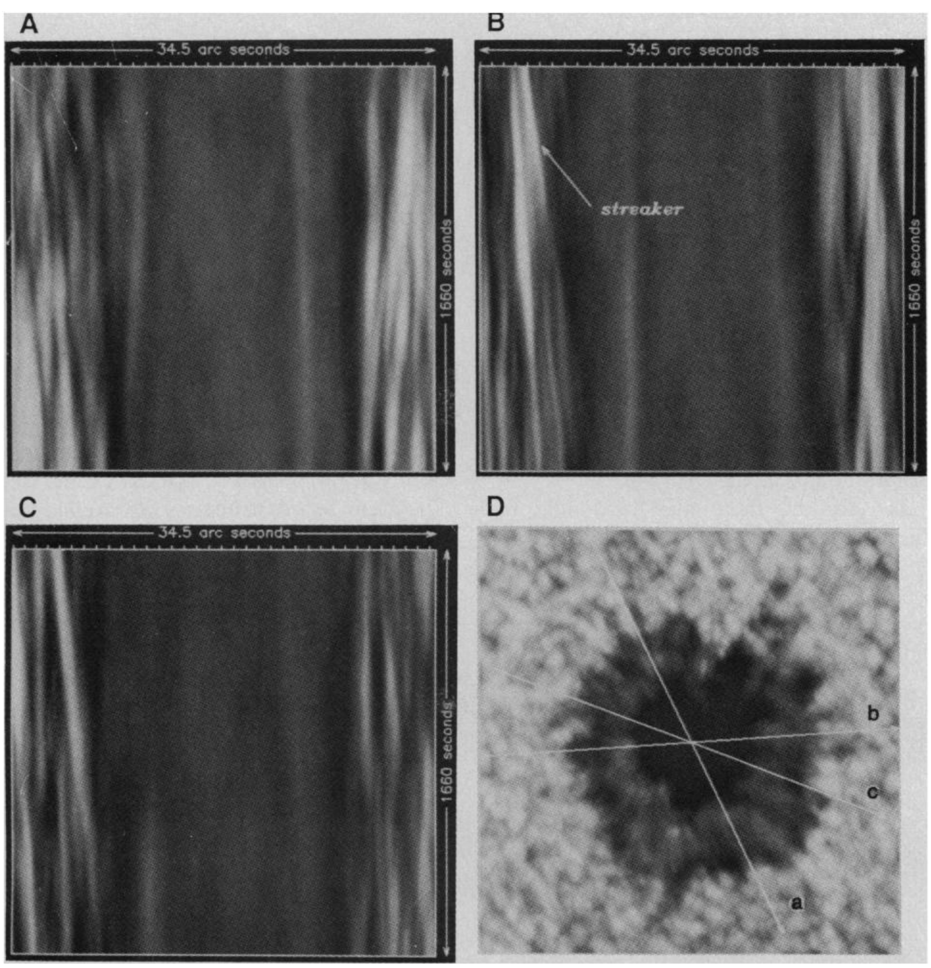

Fig. 2. (**A**, **B**, and **C**) Space-time slices (with time increasing vertically) through the sunspot with the spatial sections indicated in (**D**), which is an image at the center of the time range. These are called radial slices because the spatial sections are along a line passing through the center of the spot.

Our analysis has benefited greatly from use of an interactive video viewing system and from a number of image-processing techniques, including three-dimensional Fourier filtering. By using an optical video disk recorder and player, we can record large numbers of computer-generated images that can then be played back interactively as movie loops or single frames. Although most of the phenomena described in this report can be recognized in the raw digitized data, some would not have been discovered without viewing processed movies. The Fourier filtering enabled us to suppress the effects of solar oscillations (*2*), remove noise in the data, and enhance or suppress motions within any desired velocity range. The SOUP data analysis seems to be the first major application of these techniques for processing movies of solar events. These movies are useful tools that we expect to see used extensively in the future in spite of the demands they make on computer time and storage.

The area immediately surrounding the sunspot penumbra shows a radial outflow that is clearly visible even in the unprocessed movies, especially when viewed at high speed (600 times real time). The apparent width of this "collar flow" is ≈5 arc sec. Movies filtered to remove the pressure-mode (*p*-mode) and fundamental-mode oscillations (*2*) show the motion more clearly and allow us to estimate the velocities of individual granules, which range from 0.2 to 1.5 km/sec. The most convincing displays are the radial time slices through the sunspot in Fig. 2, which shows the intensity along lines through the center of the sunspot versus time as an image. The radially advecting granules appear as slanted lines, and the radial velocity can be determined from the slope. These proper motions have, to our knowledge, not been previously reported although their Doppler signature would explain observations of outflows beyond the penumbra in studies by Kinman (*3*) and Sheeley and Bhatnagar (*4*). Because the flow around the penumbra had lower velocities and because of pattern similarities in their Doppler images, Sheeley and Bhatnagar suggested that the flows were more closely related to the pattern of supergranulation than to the penumbral Evershed effect. This belief is consistent with the SOUP observations.

The relation of these motions to the Evershed effect is unclear although both represent radially outward flows. The moving granules could be upward convention deflected by the slanted magnetic field under the photosphere or part of a large-scale

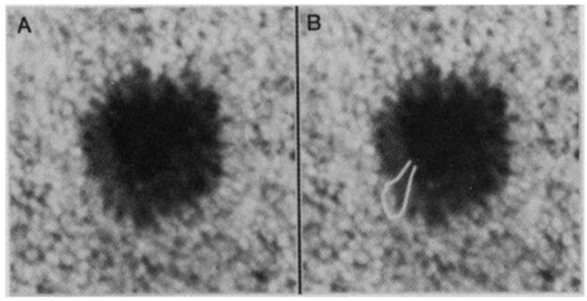

Fig. 3. (**A**) A single frame from a movie filtered to enhance motions with phase velocities between 2 and 4 km/sec. The field of view is 31,000 km. (**B**) The same image with a white line drawn to show a faint bubble or loop that seemed to be ejected from the penumbra.

convection pattern around the sunspot. It is generally accepted that the Evershed effect is concentrated in dark penumbral filaments (*5, 6*) and that the velocities end abruptly at the penumbral boundary (*7*). These dark penumbral filaments may be elevated compared to the surrounding photosphere (*8*). Actually, the granulation advection reported here is probably the source of confusion over whether the Evershed effect actually ends abruptly at the penumbra. The granular motion may or may not show up in an individual spectrum, but it would clearly be present in an average spectrum or under inferior observation conditions.

Around the penumbra there are bright, granule-like features that seem to be ejected from the sunspot penumbral boundary into the photosphere. The most obvious of these bright features, dubbed the "streaker," travels at about 2.7 km/sec. The normal granulation outflow is at one-third to one-half that rate. Thus, the bright, moving features move through (perhaps as a wave) or over the granulation. The radial trajectory of the streaker is shown in Fig. 2B, one of the time slices through the sunspot. A dark structure appears to originate in conjunction with the streaker and moves in the opposite direction into the penumbra. The streaker approaches another bright photospheric structure that is also moving outward from the spot at 1 km/sec. Another streaker is seen in Fig. 2C. We have not yet made a thorough study of these bright structures; however, they are related to activity of the nearby penumbra.

An interesting feature was noted by examining movies of images such as the one in Fig. 3. This is one frame in a movie with velocities in the range of 2 to 4 km/sec enhanced by three-dimensional Fourier filtering. This image was obtained by multiplying the appropriate Fourier coefficients by 2. A large loop or bubble that seems to be associated with two bright penumbral filaments is seen; it begins in the penumbra and travels out into the surrounding photosphere. Although it is much easier to see in Fig. 3, the same structure is visible in the raw images. We have no information on the height of this structure in the atmosphere, but it may be easier to understand energetically if it represents an ejected mass above the photosphere.

It is evident from the movies, and from images separated in time by more than 5 or 10 minutes, that some penumbral filaments or groups of filaments extend and contract at rates of 0.1 to 0.5 arc sec/min (1.2 to 6 km/sec). These expansions and contractions might be actual motions of filaments or possibly waves propagating through the filaments that cause temperature or density changes affecting the filament's visibility. These waves might be photospheric p-mode oscillations or waves generated from the umbra that then propagate along the filament. The overall impression is that the filaments overlay the surrounding photosphere, and the idea of an overlying penumbra seems more consistent with these rapid fluctuations. The areas showing the most obvious changes are marked in Fig. 1B.

Often, as precursors to the filament extensions, there are photospheric brightenings in the boundaries of the regions into which the filaments extend. This brightening is consistent with a wave scenario in which a particularly high amplitude p-mode oscillation (these have a typical spatial coherence of 10 arc sec or more) causes the photosphere to brighten and subsequently causes the density in a nearby overlying filament to increase (thereby increasing its opacity and making it appear darker).

In addition, there may be longer but fainter extensions of some filaments of tens of arc seconds, such as those indicated in Fig. 1, which are very faint and variable in visibility. It is unclear if they are above or within the photospheric granulation, but we favor the former position. Their variable visibility could be the same mechanism for the shorter extensions, that is, large-scale pressure waves. The extensions may be similar to a larger class of variable linear and arclike structures seen in the data, all of which may be density increases in overlying magnetic flux tubes.

Flow maps made by local correlation tracking (*9*) indicate that the entire penumbra flows radially outward with velocities in the range of 100 to 400 m/sec. However, this result, which is smaller than typical Doppler measurements of the Evershed flow, is affected by the field of view of the correlation tracker algorithm (4 arc sec full width at half maximum). It therefore represents an average over the penumbral structures and is probably also affected by the granulation outflow outside the penumbra. The preliminary map shows a positive divergence in the region of the penumbra. Not all of the penumbral structures move outward; some bright features are observed to move inward.

The bright penumbral grains, at least those which are inside a radius equal to 0.75 of the penumbral radius, move inward toward the umbra. The rates are up to 500 m/sec and tend to increase as the grain approaches the umbra. This rate is in agreement with earlier measurements of the motions of bright penumbral grains (*10*). A mosaic of images showing a 10 arc sec by 10 arc sec area of the penumbra and containing some moving penumbral grains is shown in Fig. 4.

Both movies and time slices show dark penumbral clouds that move outward. An area that shows particularly prominent clouds in the movies is marked in Fig. 1B. These are broad structures covering a few arc seconds, much larger than the width of

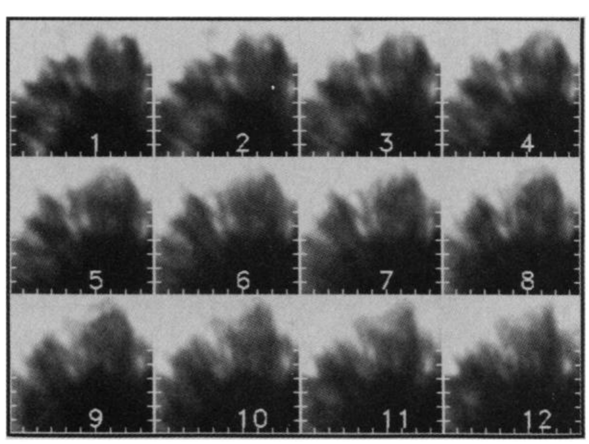

Fig. 4. A series of images showing time variations in a portion of the penumbra. The frames are 2 minutes apart, and the tick marks are spaced at 1-arc-sec intervals.

the filaments and grains. They might be related to the "dark puffs" seen in the blue wing of H_α (*11*) and to running penumbral waves, or both.

These space-based high-resolution movies of a sunspot have been successful in elucidating sunspot phenomena, and they highlight the severe handicap imposed by terrestrial atmospheric turbulence on visible-light solar observations. These data are only a hint of what can be done with a stabilized solar telescope in space. Further space-based observations coupled with image processing systems capable of handling large amounts of data will revolutionize solar physics and our understanding of stellar atmospheres.

REFERENCES AND NOTES

1. A. M. Title *et al.*, *Adv. Space Res.* **6**, 253 (1986).
2. Movies made from the raw data show strong brightness fluctuations with spatial and temporal scales characteristic of *p*-mode oscillations (that is, larger than 5000 km and about 5 minutes); these fluctuations make it difficult to follow the evolution of smaller structures. A review on solar oscillations is given by J. Christensen-Dalsgaard, D. Gough, and J. Toomre [*Science* **229**, 923 (1985)]. The SOUP data did not have sufficient resolution in Fourier space to resolve individual *p*-mode ridges; we were able to distinguish the fundamental mode, however.
3. T. D. Kinman, *Mon. Not. R. Astron. Soc.* **112**, 425 (1952).
4. N. R. Sheeley and A. Bhatnagar, *Sol. Phys.* **19**, 338 (1971).
5. J. M. Beckers, *ibid.* **3**, 258 (1968).
6. H. I. Abdusamatov and V. A. Krat, *ibid.* **14**, 132 (1970).
7. E. Wiehr, G. Stellmacher, M. Knölker, H. Grosser, *Astron. Astrophys.* **155**, 402 (1986).
8. R. L. Moore, in *Proceedings of the Physics of Sunspots*, Sunspot, NM, 14 to 17 July 1981, L. E. Cram and J. H. Thomas, Eds. (available from Sacramento Peak Observatory, Sunspot, NM), pp. 259–311.
9. L. J. November, G. W. Simon, T. D. Tarbell, A. M. Title, S. H. Ferguson, in *Proceedings of the Second Workshop on Problems in High Resolution Solar Observations*, Boulder, CO, 15 to 17 September 1986, R. G. Athay, Ed. (National Center for Atmospheric Research, Boulder, CO, in press).
10. R. Muller, *Sol. Phys.* **48**, 101 (1976).
11. R. L. Moore and F. Tang, *ibid.* **41**, 81 (1975).
12. We thank the additional members of the SOUP team for their contributions: L. Acton, D. Duncan, S. Ferguson, M. Finch, Z. Frank, G. Kelly, R. Lindgren, M. Morrill, T. Pope, R. Reeves, and R. Rehse (Lockheed Palo Alto Research Laboratory); G. Simon (Air Force Geophysics Laboratory, Sunspot, NM); J. Harvey, J. Leibacher, and W. Livingston (National Solar Observatory, Tucson, AZ); and L. November and J. Zirker (National Solar Observatory, Sunspot, NM). Supported by NASA contracts NAS8-32805 and NAS5-26813 and by the Lockheed Independent Research Fund.

26 May 1987; accepted 17 September 1987

Ultraviolet Observations of Solar Fine Structure

KENNETH P. DERE, JOHN-DAVID F. BARTOE,
GUENTER E. BRUECKNER, JOHN W. COOK, DENNIS G. SOCKER

The High Resolution Telescope and Spectrograph was flown on the Spacelab-2 shuttle mission to perform extended observations of the solar chromosphere and transition zone at high spatial and temporal resolution. Ultraviolet spectroheliograms show the temporal development of macrospicules at the solar limb. The C IV transition zone emission is produced in discrete emission elements that must be composed of exceedingly fine (less than 70 kilometers) subresolution structures.

THE NAVAL RESEARCH LABORATORY High Resolution Telescope and Spectrograph (HRTS) was one of four instruments to perform solar observations during the Spacelab-2 shuttle mission, which flew from 29 July to 6 August 1985. The HRTS instrument is well suited to study the fine structure and dynamics of the solar chromosphere and transition zone by means of ultraviolet (UV) spectroscopy. We report results from analyses of some of the significant data sets from among the large number of UV spectra and spectroheliograms that were obtained during the Spacelab-2 mission.

The HRTS is a 30-cm Gregorian telescope that produces an image of the sun on the spectrograph slit jaws with arc-second resolution. The focal-plane instrumentation consists of a tandem-Wadsworth UV spectrograph, a broadband UV spectroheliograph, and an Hα system. The spectrograph produces stigmatic photographic spectra of the slit, which has an equivalent length of 1 solar radius, a width of 0.5 arc sec and a corresponding spectral resolution of 50 mÅ throughout the 1200- to 1700-Å wavelength range. The broadband UV spectroheliograph uses a double-grating zero-dispersion broadband filter to photographically record the image reflected from the slit jaws. The Hα video image of the slit jaws is displayed on the shuttle aft flight deck for target selection and telescope focusing and is also recorded for analysis after the flight.

A broadband UV spectroheliograph image of the solar limb observed during Spacelab-2 is shown in Fig. 1. This figure shows an image of the sun reflected from the two spectrograph slit jaws with the slit roughly tangent to the solar limb and three slit jaw fiducial wires running perpendicular to the slit. The UV reflectivity of the upper slit is about four times as high as the lower slit, and this accounts for the discontinuity in the intensity of the image at the slit. The UV spectroheliograph images a band of the solar spectrum centered at 1550 Å with about a 90-Å (full width at half-maximum) passband. In this spectral region there are strong transition zone lines of C IV at 1548 and 1550 Å. There are also numerous chromospheric lines of ions such as C I, Si I, Si II, and Fe II, as well as the continuum formed at 4300 to 4900 K in the temperature minimum region. On the solar disk, the spectroheliograph integrates all of the line and continuum components in the passband, and the image shows typical upper chromospheric structures such as bushes of spicules at the supergranular cell boundaries. Above the limb the emission becomes dominated by the C IV transition zone lines.

The UV limb images show at least three categories of structures: (i) spicules similar in appearance and size to Hα spicules, (ii) larger spicular structures called macrospicules, and (iii) nested loops of transition zone plasmas, which show highly dynamic behavior. When these images are compared with near simultaneous Hα images, it can be determined that a large number of individual UV spicular structures are direct extensions of some of the larger and more distinct Hα spicules. The C IV macrospicules have

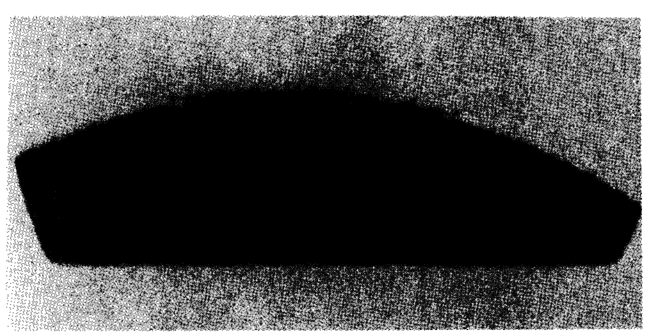

Fig. 1. Ultraviolet spectroheliograph images of C IV spicular structures at the solar limb. The distance between fiducial wires is 206 arc sec.

E. O. Hulburt Center for Space Research, Naval Research Laboratory, Washington, DC 20375.